SCIENTIFIC REPORTS

OPEN

SUBJECT AREAS:
NEURAL CIRCUIT
TISSUE ENGINEERING

Received
16 January 2014

Accepted
7 August 2014

Published
28 August 2014

Correspondence and requests for materials should be addressed to H.-C.Z. (zhaohc@mail.tsinghua.edu.cn) or L.-H.J. (l.h.jiang@leeds.ac.uk)

* These authors contributed equally to this work.

Stiff substrates enhance cultured neuronal network activity

Quan-You Zhang[1,2]*, Yan-Yan Zhang[1]*, Jing Xie[1], Chen-Xu Li[3], Wei-Yi Chen[2], Bai-Lin Liu[1], Xiao-an Wu[1], Shu-Na Li[4], Bo Huo[4], Lin-Hua Jiang[5,6] & Hu-Cheng Zhao[1]

[1]Institute of Biomechanics and Medical Engineering, Department of Engineering Mechanics, Tsinghua University, China, [2]College of Mechanics, Taiyuan University of Technology, China, [3]Medical School, Datong University, China, [4]Biomechanics and Biomaterials Laboratory, Department of Applied Mechanics, School of Aerospace Engineering, Beijing Institute of Technology, China, [5]School of Biomedical Sciences, University of Leeds, United Kingdom, [6]Department of Physiology and Neurobiology, School of Basic Medical Sciences, Xinxiang Medical University, China.

The mechanical property of extracellular matrix and cell-supporting substrates is known to modulate neuronal growth, differentiation, extension and branching. Here we show that substrate stiffness is an important microenvironmental cue, to which mouse hippocampal neurons respond and integrate into synapse formation and transmission in cultured neuronal network. Hippocampal neurons were cultured on polydimethylsiloxane substrates fabricated to have similar surface properties but a 10-fold difference in Young's modulus. Voltage-gated Ca^{2+} channel currents determined by patch-clamp recording were greater in neurons on stiff substrates than on soft substrates. Ca^{2+} oscillations in cultured neuronal network monitored using time-lapse single cell imaging increased in both amplitude and frequency among neurons on stiff substrates. Consistently, synaptic connectivity recorded by paired recording was enhanced between neurons on stiff substrates. Furthermore, spontaneous excitatory postsynaptic activity became greater and more frequent in neurons on stiff substrates. Evoked excitatory transmitter release and excitatory postsynaptic currents also were heightened at synapses between neurons on stiff substrates. Taken together, our results provide compelling evidence to show that substrate stiffness is an important biophysical factor modulating synapse connectivity and transmission in cultured hippocampal neuronal network. Such information is useful in designing instructive scaffolds or supporting substrates for neural tissue engineering.

It is well-known that all types of cells are able to detect and respond to extracellular and intracellular chemical signals. Recent studies have evidence to suggest many cells including neurons in the brain are also equipped to sense mechanical cues from their microenvironments such as the stiffness or rigidity of extracellular matrix or cell-supporting substrates, and result in profound effects on their morphology and function[1–14]. For instance, substrates with stiffness similar to brain tissues prefer to stimulate neuronal over glial growth in cortical neuronal cultures[2]. The mechanical property of neuron-supporting substrates also exerts considerable influence on important neuronal behaviors; taking hippocampal neurons for example, stiff substrates promote dendrite arborization and, by contrast, soft substrates render weak adhesion that assists neurite outgrowth and/or retraction and thereby increase the frequency of extension-retraction events and neuronal dynamics[4,5,8]. Furthermore, there is increasing evidence to suggest that the physical properties of substrates can tune synapse formation and strength in cultured neuronal network although the underlying mechanisms are not fully understood[4–7,9,13,14]. Brain injury or neurodegenerative disease can change local or global stiffness of the brain tissues, for example, local tissue stiffness is likely to increase after injury, as a result of formation of structures such as glial scars, and decrease in the brain tissues of patients with Alzheimer's disease and multiple sclerosis[15]. These and other studies have led to recognition of the mechanical property as an important factor in designing instructive scaffolds for neural tissue engineering[10–12]. A clear understanding of how the mechanical property of neuron-supporting substrates influences neuronal function is still lacking but important in inspiring a full insight into brain function and in particular development of novel neuron-supporting scaffolds for neural tissue engineering or regeneration[7,10,12–15]. We carried out the present study to investigate the effects of substrate stiffness on Ca^{2+} signaling, synapse connectivity and transmission in cultured hippocampal neuronal network.

Results

Polydimethylsiloxane (PDMS) substrates were used in the present study as have been recently shown to have a wide range of elasticity or mechanical strength independently of surface properties and thus are highly appro-

priate for study of the mechano-sensitivity of cellular processes[16]. Indeed, our two types of PDMS substrate preparations had similar surface roughness or topography as revealed using atomic force microscopy (Fig. 1a), but a 10-fold difference in Young's modulus (46 ± 11 kPa versus 457 ± 39 kPa; n = 6) as determined using the spherical indentation method (see Materials and Methods). We referred to them from here onwards as the soft and stiff substrates, respectively. Hippocampal neurons cultured on such substrates over a period of 14–18 days showed the typical size of cell body, morphology, neurite growth and extension. Neurites grew in all directions and with varying distances, and a high proportion of them made contacts with each other in the later stage (Fig. 1b–d). Further characterization by immunofluorescent confocal microscopy using antibodies that recognize MAP2 (a neuronal marker), vesicular glutamate transporter (vGLUT1) (a marker of excitatory neurons using glutamate) or GAD67 (a maker for inhibitory neurons using γ-aminobutyric acid or GABA) shows no difference in neuron density, soma size, and percentage of excitatory and inhibitory neurons on stiff and soft substrates (Fig. 1c–e).

Cytosolic Ca^{2+} is a ubiquitous signaling molecule, and neurons express numerous Ca^{2+} signaling mechanisms that play a crucial role in determining and regulating their functional roles[17]. Voltage-gated Ca^{2+} channels mediating Ca^{2+} influx into the presynaptic terminals are particularly important for synaptic transmission[17,18]. Thus, we firstly examined the effect of substrate stiffness on voltage-gated Ca^{2+} channels in hippocampal neurons in culture for 8–10 days *in vitro* (DIV8–10), using whole-cell patch-clamp recording and Ba^{2+} as the charge carrier to avoid perturbance of Ca^{2+}-dependent mechanisms. Neurons cultured on both substrates responded to depolarization pulses with non-inactivating currents (Fig. 2a). The current-voltage (I-V) relationship curves were bell-shaped; the inward currents began to appear approximately at −30 mV, reached the maximum at −5 mV and reversed at +50 mV (Fig. 2b). The amplitude of inward currents in the voltage range from −15 mV to +15 mV was significantly greater in neurons on stiff substrates as compared to that in neurons on soft substrates (Fig. 2b). Similar increases in voltage-gated Ca^{2+} channel currents in nerve growth factor-differentiated PC12 pheochromocytoma cells (Fig. 2c–d), a cell model for neuronal function. Taken together, these results suggest up-regulation of neuronal voltage-gated Ca^{2+} channels by stiff substrates.

Hippocampal neurons as they mature *in vivo* or *in vitro* develop spontaneous oscillations in the cytosolic Ca^{2+} concentrations

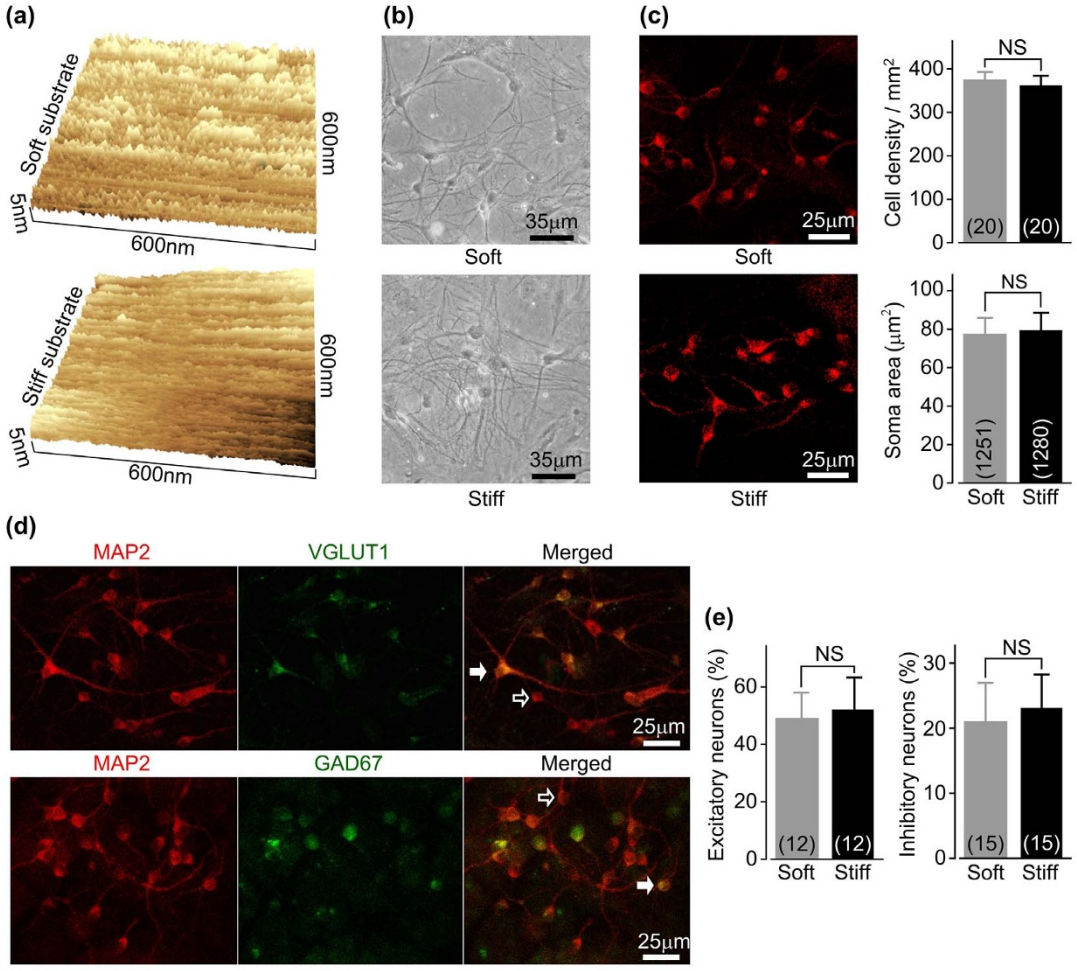

Figure 1 | Surface topography of PDMS substrates and effect of substrate stiffness on neuronal cultures. (a) Representative AFM images showing similar surface topography of soft and stiff substrates. (b) Representative optical microscopic photos showing DIV14 neurons on soft and stiff substrates. (c) *Left*: representative fluorescent confocal images showing neurons stained with MAP2. *Right*: summary of neurons density (top) and soma size (bottom), determined from images like the one shown on the left. (d) Representative MAP2 staining, GAD67 staining and merged fluorescent images (top), or MAP2 staining and vGLUT1 staining and merged fluorescent images (bottom), on soft substrates. The arrows in the merged images highlight example neurons with positive (filled) and negative (empty) co-staining. (e) Percentage of vGLUT1-positive (top) and GAD67-positive neurons (bottom). The numbers shown in parenthesis indicate images (cell density in (c) and (e)) or neurons (soma area in (c)) examined in each case. Similar results were observed in four independent experiments. NS denotes no significant difference.

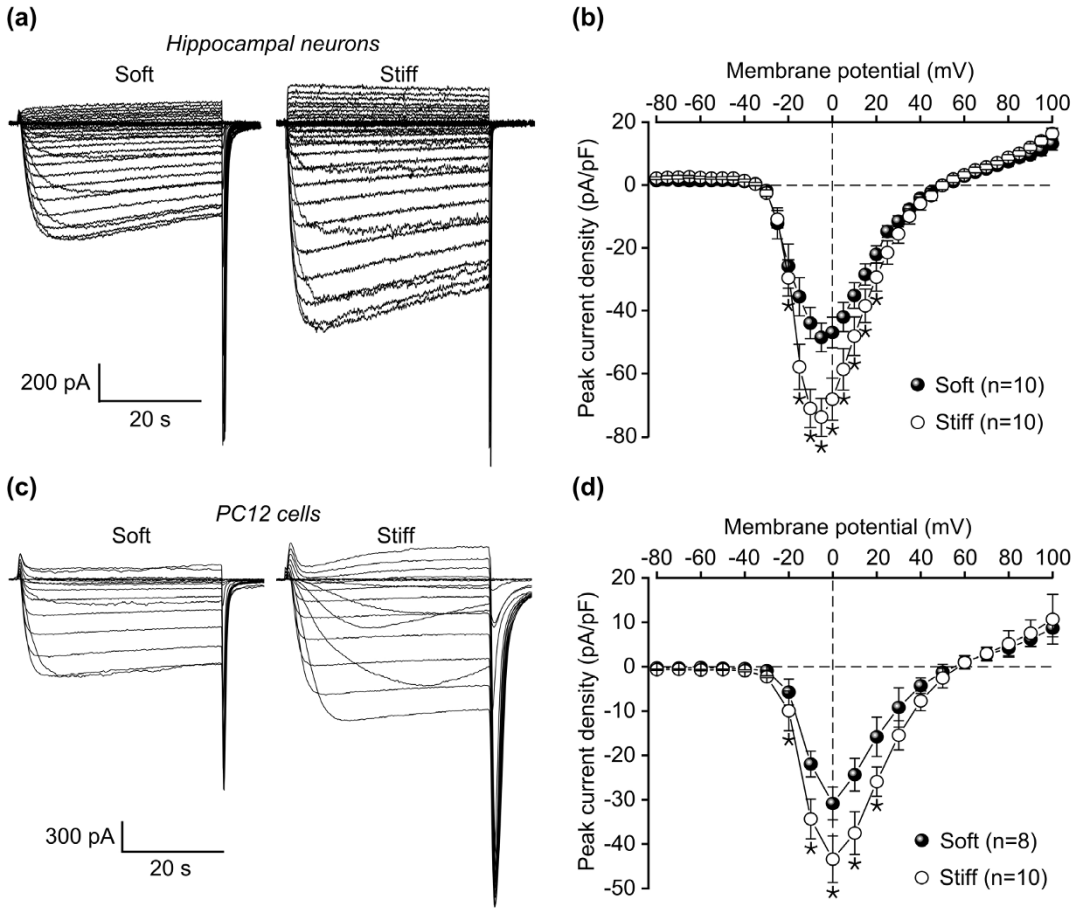

Figure 2 | Stiff substrate enhances voltage-gated Ca^{2+} channel currents in hippocampal neurons and PC12 cells. (a) Representative whole-cell Ba^{2+} current recordings from DIV8–10 neurons on soft and stiff substrates. (b) Mean I-V relationship curves from recordings of 10 neurons from three preparations. (c) Representative whole-cell Ba^{2+} current recordings from PC12 neurons cultured for 8–10 days on soft and stiff substrates. (d) Mean I-V relationship curves. The number of cells recorded in each case is shown in parenthesis. *, $p < 0.05$ denotes difference in the current density at the same membrane potential.

($[Ca^{2+}]_c$), or Ca^{2+} oscillation as a result of synapse formation in neuronal network[19–24]. We combined time lapse microscopy and Fura-2 ratiometry to investigate the effect of substrate stiffness on basal $[Ca^{2+}]_c$ and Ca^{2+} oscillation in DIV14-18 neurons (Fig. 3a–c). The basal $[Ca^{2+}]_c$ were similar in neurons cultured on soft and stiff substrates (Fig. 3d). Ca^{2+} oscillations were observed in a majority of neurons but neurons on stiff substrates exhibited significant increases in both frequency and amplitude (Fig. 3e–f) with no discernible change in synchronization (Fig. 3g).

Ca^{2+} oscillations have been shown to be mediated by excitatory and inhibitory neurons or synapses in the neuronal networks[19–22]. To further study the effects of substrate stiffness on synapse formation and function, we recorded spontaneous excitatory and inhibitory postsynaptic currents (sEPSC and sIPSC) from DIV14–18 neurons. The results are summarized in Fig. 4. There were significant increases in both amplitude and frequency of sEPSC in neurons on stiff substrates (Fig. 4b–c) and by contrast no effect on sIPSC was detected (Fig. 4e–f). We also determined the synaptic connectivity directly by paired recording (Fig. 5a) on the basis that action potentials (APs), induced by injecting currents into one (or presynaptic) neuron, evoke neurotransmitter release and subsequent postsynaptic currents in another synaptically coupled (postsynaptic) neuron. The average percentage of synaptic connectivity among neurons on stiff substrates was significantly greater than that among neurons on soft substrates (Fig. 5b). More specifically, stiff substrates increased both excitatory and inhibitory synaptic connectivity (Fig. 5c). All the synaptic connectivity was completely abolished in extracellular Ca^{2+}-free solutions (data not shown), consistent with a critical role of Ca^{2+} influx in inducing synaptic transmission. We also examined the electrical coupling between neurons. The prevalence of electrical coupling and the coupling coefficient were not altered by substrate stiffness (Fig. 5d–f). Finally, we compared AP-evoked excitatory postsynaptic currents (EPSC) and inhibitory postsynaptic currents (IPSC), and also paired-pulse facilitation (PPF) or depression (PPD) that are often indicative of vesicular release probability (Pr) of neurotransmitters with a lower Pr resulting in a greater PPF or PPD value[25]. The cumulative distribution of postsynaptic currents shows that the size of evoked EPSC was increased significantly in neurons on stiff substrates relative to that in neurons on soft substrates (Fig. 5g). The PPF value was, as expected, significantly lower for neurons on stiff substrates (1.12 ± 0.07) than on soft substrates (1.38 ± 0.08; $p < 0.05$) (Fig. 5h), consistent with enhanced excitatory synaptic transmission. In contrast, there was no change in evoked IPSC and PPD value (Fig. 5i–j). Collectively, these results provide consistent evidence to show that stiff substrates preferentially enhance the excitatory synaptic connectivity and transmission in cultured hippocampal neuronal network.

Discussion

The present study provides evidence to show that substrate stiffness strongly enhances voltage-gated Ca^{2+} channel currents, Ca^{2+} oscillations, synaptic connectivity, and excitatory neurotransmission in cultured hippocampal neuronal networks.

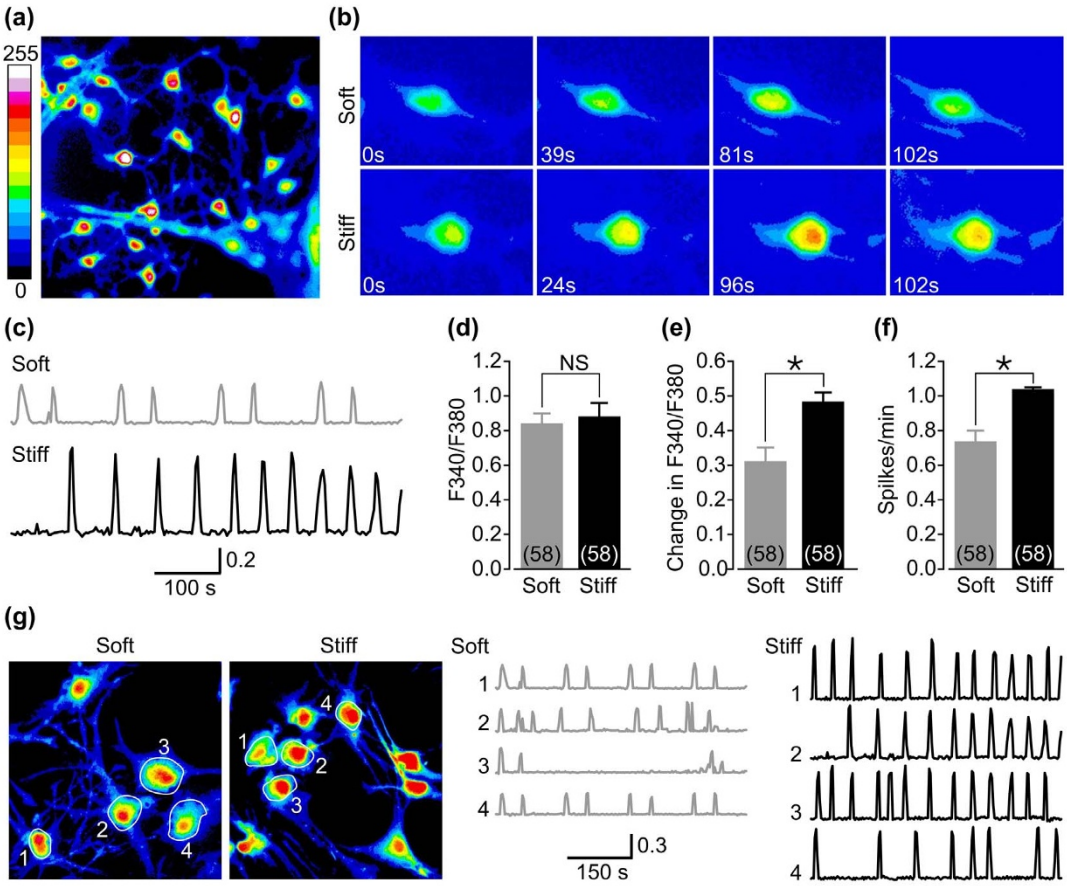

Figure 3 | Stiff substrate increases synchronized spontaneous cytosolic Ca^{2+} oscillations in cultured neural networks of hippocampal neurons. (a) Representative single cell images showing Ca^{2+} fluorescence in DIV14–18 neurons on stiff substrates. (b) Representative single cell images showing Ca^{2+} fluorescence intensity at given time points from one neuron on soft substrate and another neuron on stiff substrate. (c) Representative time elapse recordings of Ca^{2+} oscillations from neurons on soft and stiff substrates. (d) Summary of the basal cytosolic Ca^{2+} concentrations (left), and the magnitude (middle) and frequency (right) of Ca^{2+} oscillations in 58 neurons on soft and stiff substrates from three preparations. *, $p < 0.05$ denotes significant difference, and NS, no significant difference. (g) *Left*: representative single cell images showing Ca^{2+} fluorescence in DIV14–18 neurons on soft and stiff substrates. *Right*: time elapse recordings of Ca^{2+} oscillations from four neurons as denoted by circles in the left images.

As mentioned above, neurons express a diversity of Ca^{2+} signaling mechanisms that are important for brain functions[17,18,25–27], including presynaptic voltage-gated Ca^{2+} channels to mediate transmission at synapses, and synchronized Ca^{2+} oscillations in neuronal networks to determine neuronal plasticity. Diverse extrinsic chemical signals and intrinsic mechanisms exist at both presynaptic and postsynaptic sites to determine or modulate synaptic formation and transmission[17,22–28]. For example, expression of cadherin-9 is crucial for synapse formation between dentate gyrus and CA3 neurons in hippocampus[28] and neuropeptides via activation of distinctive G-protein-coupled receptors can alter the amplitude and/or frequency of Ca^{2+} oscillations and thereby neuronal plasticity[23]. Emergent evidence suggests that the physical properties of neuron-supporting substrates are also influential. Thus, culturing neuronal stem cell-differentiated neurospheres on graphene, as opposed to tissue culture plastic surface, enhanced synchronized spontaneous Ca^{2+} oscillations and postsynaptic currents[14]. Stretching the membranes which supported cortical neurons significantly reduced spontaneous Ca^{2+} oscillations and excitatory postsynaptic currents[29]. The present study examined hippocampal neurons cultured on substrates with different stiffness, and revealed that the stiff substrates significantly up-regulated Ca^{2+} signaling mechanisms, including voltage-gated Ca^{2+} channels (Fig. 2) and synchronized spontaneous Ca^{2+} oscillations (Figs. 3). More importantly, our study has shown that the stiff substrates enhanced synaptic connectivity and excitatory synaptic transmission (Figs. 4–5). To our best knowledge, this is the first study to show that neurons can sense mechanical cues from their microenvironments and integrate into synapse connectivity and transmission. The increases in both Ca^{2+} channel activity (Fig. 2) and synaptic connectivity induced by the stiff substrates (Fig. 5b), and no detectable synaptic connectivity in extracellular Ca^{2+}-free solutions support the importance of Ca^{2+} signalling or presynaptic Ca^{2+} influx through voltage-gated Ca^{2+} channels. The stiff substrates also stimulated synchronized spontaneous Ca^{2+} oscillations in cultured neuronal network (Fig. 3), and facilitated excitatory synaptic connectivity and transmission (Fig. 4a–c, Fig. 5c and Fig. 5g–h). These findings are consistent with the notion that the Ca^{2+} oscillations result from periodic burst firing of APs engaging excitatory synaptic transmission via activation of L-type voltage-gated Ca^{2+} channels and excitatory NMDA receptors[19,22,23,30]. The excitatory $GABA_A$ receptors in the neonatal hippocampus have been reported to mediate the Ca^{2+} oscillations in synergy with NMDA receptors[19]. This study has shown that the stiff substrates also enhanced the inhibitory synaptic connectivity (Fig. 5c) but did not alter the inhibitory synaptic transmission (Fig. 4d–f and Fig. 5i–j). Further investigations are required to determine the contribution of the excitatory and inhibitory receptors in mediating the increases in the Ca^{2+} oscillations and the discriminating effects on the excitatory versus inhibitory synaptic transmission. The increases in spontaneous Ca^{2+} oscillations on stiff substrates have also been documented in other cell types; for

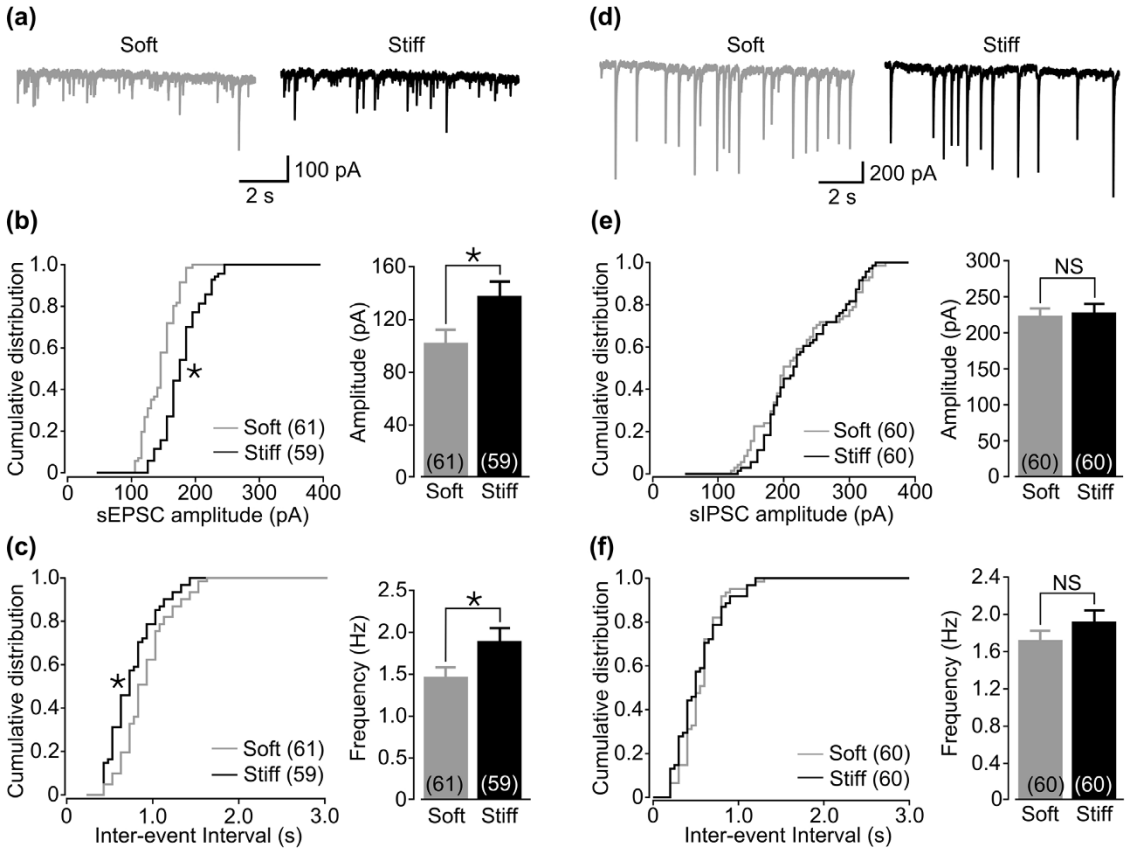

Figure 4 | Effects of substrate stiffness on spontaneous EPSC and IPSC. (a) Representative recordings of spontaneous EPSC from DIV14–18 neurons in soft and stiff substrates. (b) Cumulative distribution and amplitude of spontaneous EPSC. (c) Cumulative distribution of inter-event intervals and frequency of spontaneous EPSC. (d) Representative recordings of spontaneous IPSC from DIV14–18 neurons in soft and stiff substrates. (e) Cumulative distribution and amplitude of spontaneous IPSC. (f) Cumulative distribution of inter-event intervals and frequency of spontaneous IPSC. *, $p < 0.05$ denote significant difference, and NS, no significant difference. The numbers shown in parenthesis indicate neurons examined in each case.

example, spontaneous cytosolic Ca^{2+} oscillations became more frequent in human mesenchymal stem cells when cultured on stiff polyacrylamide gel substrates or were amplified in endothelial cells when migrating from soft to stiff region of the substrates[31]. It is thus attractive to propose tuning the frequency and/or amplitude of cytosolic Ca^{2+} oscillations as a common intrinsic mechanism which cells use to encode the difference and/or change in the mechanical property of their microenvironments. Neurons examined in the present study were supported directly by the substrates based on visual examination (Fig. 1b). The stiff substrates increased the voltage-gated Ca^{2+} channel currents in cultured hippocampal neurons (Fig. 2a–b) and similarly in nerve growth factor-differentiated PC12 cells (Fig. 2c–d). Taken together, these results support expression of intrinsic mechano-sensing mechanisms in neurons. Nevertheless, it is worth pointing out that our hippocampal neuronal preparations like those used in many previous studies contained glial cells, and thus we cannot exclude the intriguing possibility that the glial cells have a role in sensing the mechanical cues and relaying to co-existing neurons. The PDMS substrates used in this present study are similar to those in previous studies, particularly those focusing on tissue engineering, and the substrate stiffness is much higher than the overall stiffness of brain tissues[2,15,16]. While it is important to determine the effects of changing the substrate stiffness occurring to the brain tissues on synaptic formation and function, the interesting finding reported in the present study is useful for the development of novel instructive scaffolds for neural tissue engineering.

The mechano-sensing mechanisms are currently still poorly understood, despite several cytoskeletal and signaling proteins have been identified in various cell types, including receptor-like protein tyrosine phosphatase[4], integrins[7,31–33], RhoA[34] and GAP-43[35] as well as mechano-sensitive ion channels[36]. In addition, there is evidence suggesting that the effect of substrate stiffness on dendrite arborization is mediated by glutamate receptors[30]. More investigations are clearly required to identify the neuronal voltage-gated Ca^{2+} channels that are up-regulated by stiff substrates, and particularly elucidate the mechano-sensing mechanisms that enhance voltage-gated Ca^{2+} channel function, synaptic connectivity, excitatory synaptic transmission, and synchronized spontaneous Ca^{2+} oscillations we have reported here in cultured hippocampal neuronal network.

In summary, we have shown stiffness of cell-supporting substrates can strongly modulate excitatory synaptic connectivity and transmission in cultured hippocampal neuronal network. Such findings are useful for design of instructive scaffolds to be used in neural tissue engineering as well as to inspire a new insight into brain functions and mechanisms of diseases that change extracellular matrix compliance.

Methods

Preparation and characterization of PDMS substrates. PDMS curing agent (sylgard184; Dow corning Corp) were mixed with base agent in a mass ratio of 10 : 1 or 50 : 1 in 15-ml centrifugal tubes, and centrifuged in a bench-top centrifuge to remove air bubbles. The mixture of ~100 μl was transferred using a pipette onto the top of four 12-mm coverslips in a 35-mm petri dish and left at 65°C for 12 hrs; the resulting PDMS substrates were oxidized in an oxygen plasma cleaner, which generated silanol group (Si-OH) on the surface of the PDMS, then sterilized by UV radiation for 2 hrs, coated with fibronectin and left in a laminar flow cabinet for at least 2 hrs. The PDMS-coverslips were washed extensively with sterile water and dried before being used to culture hippocampal neurons as described previously[37]. The substrate surface topography was examined using atomic force microscopy (AFM) (Nanoscope IIIa system, Digital Instruments, Santa Barbara, CA, USA) in a

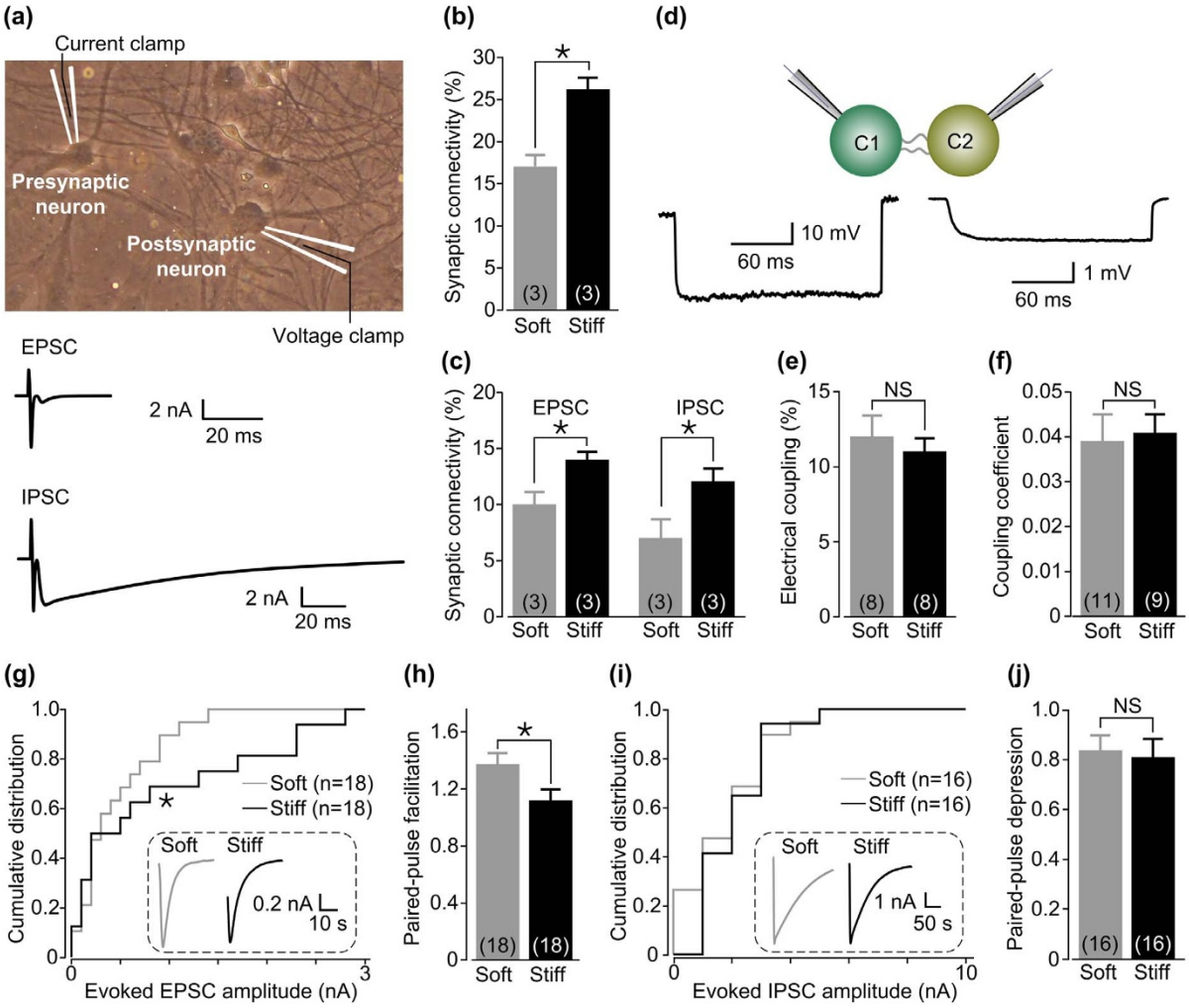

Figure 5 | Stiff substrate facilitates excitatory synaptic connectivity and transmission in the neural networks of hippocampal neurons. (a) Experimental setting of paired recording; one (presynaptic) neuron was stimulated by the electrode in current-clamp configuration to evoke APs and the unitary postsynaptic currents in the other (postsynaptic) neuron were detected by the electrode in voltage-clamp configuration. Example unitary EPSC and IPSC with distinct kinetics are illustrated at the bottom. (b) Summary of percentage of pairs of neurons that exhibited synaptic connectivity or transmission on soft and stiff substrates. In total, 181 pairs of neurons on soft and stiff substrates each from three independent preparations respectively were examined. (c) Summary of the percentage of pairs of neurons on soft and stiff substrates that showed excitatory and inhibitory synaptic connectivity (from (b)). (d) Paired recording from a pair of electrically coupled neurons. The experimental protocol is illustrated on top: a hyperpolarizing step current was injected to the presynaptic neuron C1, and changes in membrane potential were recorded from both presynaptic neuron and postsynaptic neuron (C2). Representative recordings of changes in membrane potential in C1 and C2 cells are shown below. (e) Summary of the percentage of electrically coupled neurons on soft and stiff substrates. In total, 54 pairs of neurons on soft substrates and 46 pairs of neurons on stiff substrates from 8 independent preparations were examined. (f) Summary of the coupling coefficient values for electrically coupled neurons. (g) The cumulative distribution of AP-evoked EPSC recorded in 18 neurons from seven independent preparations in each case. *Insert*: evoked EPSC traces from neurons on soft and stiff substrates. (h) Mean PPF value for 18 neurons on soft and stiff substrates from seven independent preparations. (i) The cumulative distribution of AP-evoked IPSC recorded in 16 neurons from seven independent preparations. *Insert*: evoked IPSC traces in neurons on soft and stiff substrates. (j) Mean PPD value for 16 neurons on soft and stiff substrates each from seven independent preparations. The numbers shown in parenthesis indicate neuron preparations (b–c and e) or neurons examined (f–j) in each case. *, $p < 0.05$ denotes significant difference, and NS, no significant difference.

tapping mode with 512 × 512 pixel data acquisition and 1 Hz scan speed. The AFM images were recorded with a standard silicon tip on a cantilever beam. The cantilever had a spring constant of 50 pN/nm, and was 125 μm long with a resonant frequency of 300 kHz.

The Young's modulus of the substrates was determined using the spherical indentation method and ElectroForce®3100 test instrument (Bose, Shanghai, China) as described previously[38]. In brief, the samples had a diameter of 55 mm and a height of 15 mm. The spherical indenter of 3-mm radius was used. The loading procedures were undertaken with controlled displacement, and the loading rate was set at 2 mm/s and the maximum indentation depth at 3 mm. Measurements were undertaken at six different positions of the sample, and the depth-indentation load curves were recorded. The initial shear modulus was determined by fitting the load curves up to different ratios of h/R using the following equation: $P = \frac{16}{9} E\sqrt{Rh}h\left(1 - 0.15\frac{h}{R}\right)$, where P represents indentation load, E Young's modulus, h indentation depth and R indenter radius[38].

Hippocampal neuron culture preparation and PC12 cell culture. All animal procedures were in accordance with the guidelines approved by Tsinghua University. Mouse hippocampal neurons were isolated from one day old pups as previously described[18,39]. In brief, after the blood vessels and meninges were removed, the hippocampus was collected into tubes in cold Hank's balanced salt solution (HBSS), and rinsed twice with HBSS solutions. Tissues were digested in TrypIE (Sigma) for 15 min at 37°C and gently triturated using pipette tips to cell suspension in DMEM medium supplemented with 10% fetal bovine serum (FBS) and 2% B-27 (Life Technologies). Cells were seeded approximately 6000 cells/cm^2 and were maintained at 37°C in humidified atmosphere with 5% CO_2. Arabinofuranosyl cysteine at 1 μg/

ml was added to culture medium 2–3 days after initial seeding to inhibit glial proliferation. PC12 cells were seeded on substrates and culture in DMEM medium supplemented with 10% FBS and 50 ng/ml nerve growth factor (Sigma) for 8–10 days before use.

Immunofluorescence staining and confocal imaging. This was performed at room temperature except incubation with the primary antibody at 4°C. DIV14 cells were washed with phosphate buffered solutions (PBS), fixed with 4% paraformaldehyde in PBS for 15 min and then permeabilized with 0.2% Triton X-100 (Sigma) in PBS for 5 min. After extensive washing with PBS, cells were blocked with 5% bovine serum albumin in PBS for 60 min, and incubated with primary rabbit polyclonal MAP2 antibody (Abcam) at a dilution of 1 : 500 alone, or together with mouse monoclonal GAD67 antibody (Millipore) at 1 : 200 or mouse monoclonal vGLUT1 (Millipore) at 1 : 200 overnight. After extensive wash with PBS, cells were incubated with secondary Alexa Fluor568 goat anti-rabbit IgG antibody (Molecular Probes) at 1 : 1000 alone or with Alexa Fluor488 goat anti-mouse IgG antibody (Molecular Probes) at 1 : 1000 for 60 min. Fluorescence images were captured using a fluorescence microscope (TCS SP5, Leica Microsystems).

Patch-clamp recording. Whole-cell currents were recorded from DIV8–10 neurons at room temperature, using an Axopatch 200B amplifier and pClamp software version 10.0 (Axon Instruments). The patched cells were perfused at 0.5 ml/min in extracellular solution containing (in mM): 140 tetraethylammonium (TEA)-Cl, 10 $BaCl_2$, 10 HEPES and 20 glucose, pH 7.3 with TEA-OH, 310 mOsm. The pipette solution contained (in mM): 110 CsCl, 10 EGTA, 4 Mg-ATP, 0.3 Na-GTP, 25 HEPES, 10 Tris-phosphocreatine and 20 U/ml creatine phosphokinase, pH 7.3 with CsOH, 290 mOsm. The resistance of recording pipettes in extracellular solution was 3.0–4.0 MΩ. The membrane potential was held at −80 mV and series resistance compensated by 80%. Currents were evoked by applying test pulses of −75 mV to +100 mV with 40-s duration and an increment of 5 mV at 10-s intervals. The cell capacitance (32 ± 12 pF) and series resistance (<20 MΩ) were monitored throughout the recording. Signals were filtered at 1 kHz and digitized at 10 kHz. The leak currents were corrected using the online P/6 trace subtraction.

Cytosolic Ca^{2+} measurement. Cytosolic Ca^{2+} concentrations in DIV14–18 neurons were measured at room temperature using Fura-2 ratiometric method. In brief, neurons were incubated with 2 μM Fura-2/acetoxymethyl ester (Life Technologies) in DMEM culture medium at 37°C for 30 min, followed by washing three times with phosphate buffer saline. Cells bathed in MEM with 2% FBS were placed on the stage of an Olympus IX71 inverted microscope equipped with a Xenon illumination system and an IMAGO CCD camera (Till Photonics, Germany). The fluorescence, excited alternatively with 340 nm and 380 nm and emitted at 510 nm, were recorded, stored digitally and analyzed by TILLvisION 4.0 program.

Spontaneous and AP-evoked postsynaptic current recordings. Postsynaptic current recordings were made from DIV14–18 neurons. The recording chamber was perfused at 0.5 ml/min with extracellular Tyrode's solution containing (in mM): 125 NaCl, 2 KCl, 4 $CaCl_2$, 4 $MgCl_2$, 25 HEPES and 30 glucose, pH 7.3 with NaOH, 310 mOsm. The pipette solution contained (in mM): 100 KCl, 2 EGTA, 4 Mg-ATP, 0.3 Na-GTP, 30 HEPES, 10 Tris-phosphocreatine and 20 U/ml creatine phosphokinase, pH 7.3 with KOH, 290 mOsm. Spontaneous and evoked inhibitory postsynaptic currents (IPSC) were recorded in extracellular solutions containing 20 μM NBQX, and spontaneous and evoked excitatory postsynaptic currents (EPSC) in extracellular solutions containing 10 μM bicuculline. In some experiments, extracellular solutions without $CaCl_2$ were used. Spontaneous postsynaptic currents were recorded with the membrane potential held at −70 mV for 5 min. AP-evoked postsynaptic currents and paired-pulse facilitation (PPF) or depression (PPD) were determined by paired recording without capacitance compensation as previously described[18]. The presynaptic neurons were depolarized to 0 mV for 1 ms to elicit APs at 10-s intervals. The unitary postsynaptic currents were recorded from the paired postsynaptic neurons at a holding potential of −70 mV. 30 AP-evoked EPSC and IPSC were recorded from each neuron. Evoked EPSC and IPSC exhibited different decay kinetics, with average rise and decay times of 3 ± 0.3 ms and 24 ± 2.6 ms for EPSC (n = 18), and 4 ± 0.4 ms and 184 ± 12.4 ms for IPSC (n = 16), respectively. PPF was determined by evoking two EPSC at a 50-ms interval and PPD by evoking two IPSC at a 200-ms interval. To minimize the potential effects of spatial proximity on synaptic connectivity, paired recordings were made from a pair of neurons in the distance of 100–150 μm.

Electrical coupling. The electrical coupling between neurons was examined using the protocols described previously by Lefler et al[40]. A hyperpolarizing current of 300 or 500 pA was delivered to the presynaptic neuron and measured the ensuing changes in membrane potential in both neurons. The ratio of the steady-state change in membrane potential in the presynaptic neuron to that in the postsynaptic neuron was calculated as the electrical coupling coefficient (CC). The CC value of <0.002 is indicative of no electrical coupling.

Statistical analysis. The data were presented as mean ± s.e.m., where appropriate. The neuron density was derived from MAP2-positive cells that were counted in fluorescent images and converted to the number of neurons per mm^2, and the soma area of individual MAP2-positive cells was estimated, using ImageJ. The percentage of excitatory and inhibitory neurons was obtained by visually identifying the number of MAP2-positive and vGLUT1-positive neurons or MAP2-positive and GAD67-positive neurons, and divided by the number of MAP2-positive neurons examined. The peak Ba^{2+} currents were normalized to the cell membrane capacitance and presented as current density. To determine the basal Ca^{2+} level and cytosolic Ca^{2+} oscillations, cells with the basal F340/F380 value within the average ± 2 × standard deviation were included in analysis, and a Ca^{2+} spike was defined with its amplitude being >1.2 times of the basal level. The number of Ca^{2+} oscillation per minute and the changes in F340/F380 were used to calculate the frequency and amplitude. Spontaneous postsynaptic currents were analyzed using Clampfit (Molecular Devices) and Mini Analysis Progrom (Synaptosoft). The last 10 AP-evoked EPSCs and IPSCs were averaged to obtain the postsynaptic current amplitude which was used to construct the cumulative distribution as described previously[17]. PPF value was derived by the ratio of the second EPSC over the first EPSC and PPD value by the ratio of the second IPSC over the first IPSC. Statistical analysis was conducted using Student's t-test for the mean data and using Kolmogorov-Smirnov for the cumulative distribution of spontaneous and evoked EPSC and IPSC, with the difference to be considered significant at $p < 0.05$.

1. Engler, A. J., Sen, S., Sweeney, H. L. & Discher, D. E. Matrix elasticity directs stem cell lineage specification. *Cell.* **126**, 677–689 (2006).
2. Georges, P. C., Miller, W. J., Meaney, D. F., Sawyer, E. S. & Janmey, P. A. Matrices with compliance comparable to that of brain tissue select neuronal over glial growth in mixed cortical cultures. *Biophys. J.* **90**, 3012–3018 (2006).
3. Solon, J., Levental, I., Sengupta, K., Georges, P. C. & Janmey, P. A. Fibroblast adaptation and stiffness matching to soft elastic substrates. *Biophys. J.* **93**, 4453–4461 (2007).
4. Kostic, A., Sap, J. & Sheetz, M. P. RPTPα is required for rigidity-dependent inhibition of extension and differentiation of hippocampal neurons. *J. Cell. Sci.* **120**, 3895–3904 (2007).
5. Previtera, M. L., Langhammer, C. G., Langrana, N. A. & Firestein, B. L. Regulation of dendrite arborization by substrate stiffness is mediated by glutamate receptors. *Ann. Biomed. Eng.* **38**, 3733–3743 (2010).
6. Mih, J. D., Marinkovic, A., Liu, F., Sharif, A. S. & Tschumperlin, D. J. Matrix stiffness reverses the effect of actomyosin tension on cell proliferation. *J. Cell. Sci.* **125**, 5974–5983 (2012).
7. Schiller, H. B. *et al.* β1-and αv-class integrins cooperate to regulate myosin II during rigidity sensing of fibronectin-based microenvironments. *Nat. Cell. Biol.* **15**, 625–636 (2013).
8. Sur, S., Newcomb, C. J., Webber, M. J. & Stupp, S. I. Tuning supramolecular mechanics to guide neuron development. *Biomaterials.* **34**, 4749–4757 (2013).
9. Yip, A. K. *et al.* Cellular response to substrate rigidity is governed by either stress or strain. *Biophys. J.* **104**, 19–29 (2013).
10. Place, E. S., Evans, N. D. & Stevens, M. M. Complexity in biomaterials for tissue engineering. *Nat. Mater.* **8**, 457–470 (2009).
11. Previtera, M. L. *et al.* The effects of substrate elastic modulus on neural precursor cell behavior. *Ann. Biomed. Eng.* **41**, 1193–1207 (2013).
12. Fabbro, A., Bosi, S., Ballerini, L. & Prato, M. Carbon nanotubes: artificial nanomaterials to engineer single neurons and neuronal networks. *ACS Chem. Neurosci.* **15**, 611–618 (2012).
13. Cellot, G. *et al.* Carbon nanotube scaffolds tune synaptic strength in cultured neural circuits: novel frontiers in nanomaterial-tissue interactions. *J. Neurosci.* **31**, 12945–12953 (2011).
14. Tang, T. *et al.* Enhancement of electrical signaling in neural networks on graphene films. *Biomaterials.* **34**, 6402–6411 (2013).
15. Franze, K., Janmey, P. A. & Guck, J. Mechanics in neuronal development and repair. *Annu. Rev. Biomed. Eng.* **15**, 227–251 (2013).
16. Palchesko, R. N., Zhang, L., Sun, Y. & Feinberg, A. W. Development of polydimethylsiloxane substrates with tunable elastic modulus to study cell mechanobiology in muscle and nerve. *PLoS One.* **7**, e51499 (2012).
17. Berridge, M. J. Neuronal calcium signaling. *Neuron.* **21**, 13–26 (1998).
18. Cao, Y. Q. *et al.* Presynaptic Ca^{2+} channels compete for channel type-preferring slots in altered neurotransmission arising from Ca^{2+} channelopathy. *Neuron.* **43**, 387–400 (2004).
19. Leinekugel, X., Medina, I., Khalilov, I., Ben-Ari, Y. & Khazipov, R. Ca^{2+} oscillations mediated by the synergistic excitatory actions of GABA(A) and NMDA receptors in the neonatal hippocampus. *Neuron.* **18**, 243–255 (1997).
20. Bacci, A., Verderio, C., Pravettoni, E. & Matteoli, M. Synaptic and intrinsic mechanisms shape synchronous oscillations in hippocampal neurons in culture. *Eur. J. Neurosci.* **11**, 389–397 (1999).
21. Wang, X. S. & Gruenstein, E. I. Mechanism of synchronized Ca^{2+} oscillations in cortical neurons. *Brain Res.* **767**, 239–249 (1997).
22. Przewlocki, R. *et al.* Opioid enhancement of calcium oscillations and burst events involving NMDA receptors and L-type calcium channels in cultured hippocampal neurons. *J. Neurosci.* **19**, 9705–9715 (1999).
23. Liu, Z. J. *et al.* Frequency modulation of synchronized Ca^{2+} spikes in cultured hippocampal networks through G-protein-coupled receptors. *J. Neurosci.* **23**, 4156–4163 (2003).
24. Numakawa, T. *et al.* Brain-derived neurotrophic factor-induced potentiation of Ca(2+) oscillations in developing cortical neurons. *J. Biol. Chem.* **277**, 6520–6529 (2002).

25. Chen, G., Harata, N. C. & Tsien, R. W. Paired-pulse depression of unitary quantal amplitude at single hippocampal synapses. *Proc. Natl. Acad. Sci. U.S.A.* **101**, 1063–1068 (2004).
26. Atwood, H. L. & Karunanithi, S. Diversification of synaptic strength: presynaptic elements. *Nat. Rev. Neurosci.* **3**, 497–516 (2002).
27. Zucker, R. S. & Regehr, W. G. Short-term synaptic plasticity. *Annu. Rev. Physiol.* **64**, 355–405 (2002).
28. Williams, M. E. *et al*. Cadherin-9 regulates synapse specific differentiation in the developing hippocampus. *Neuron.* **71**, 640–655 (2011).
29. Goforth, P. B., Ren, J. H., Schwartz, B. S. & Satin, L. S. Excitatory synaptic transmission and network activity are depressed following mechanical injury in cortical neurons. *J. Neurophysiol.* **105**, 2350–2363 (2011).
30. Firestein, B. L., Langhammer, C. G., Langrana, L. N. & Firestein, B. L. Regulation of dendrite arborization by substrate stiffness is mediated by glutamate receptors. *Annu. Biomed. Eng.* **38**, 3733–3743 (2010).
31. Shyy, J. Y. & Chien, S. Role of integrins in endothelial mechanosensing of shear stress. *Circ. Res.* **91**, 769–755 (2002).
32. Choquet, D., Felsenfeld, D. P. & Sheetz, M. P. Extracellular matrix rigidity causes strengthening of integrin cytoskeleton linkages. *Cell.* **88**, 39–48 (1997).
33. Lin, B., Arai, A. C., Lynch, A. G. & Gall, C. M. Integrins regulate NMDA receptor mediated synaptic currents. *J. Neurophysiol.* **89**, 2874–2878 (2003).
34. Kim, T. J. *et al*. Substrate rigidity regulates Ca^{2+} oscillation via RhoA pathway in stem cells. *J. Cell. Physiol.* **218**, 285–293 (2009).
35. Li, N. *et al*. The promotion of neurite sprouting and outgrowth of mouse hippocampal cells in culture by graphene substrates. *Biomaterials.* **32**, 9374–9382 (2011).
36. Kobayashi, T. & Sokabe, M. Sensing substrate rigidity by mechanosensitive ion channels with stress fibers and focal adhesions. *Curr. Opin. Cell. Biol.* **22**, 669–676 (2010).
37. Cheng, C. M. *et al*. Probing localized neural mechanotransduction through surface-modified elastomeric matrices and electrophysiology. *Nat. Protoc.* **5**, 714–724 (2010).
38. Zhang, M. G., Cao, Y. P., Li, G. Y. & Feng, X. Q. Spherical indentation method for determining the constitutive parameters of hyperelastic soft materials. *Biomech. Model. Mechanobiol.* (doi 10.1007/s10237-013-0481-4) (2013).
39. Beaudoin, G. M. *et al*. Culturing pyramidal neurons from the early postnatal mouse hippocampus and cortex. *Nat. Protoc.* **7**, 1741–1754 (2012).
40. Lefler, Y., Yarom, Y. & Uusisaari, M. Y. Cerebellar inhibitory input to the inferior olive decreases electrical coupling and blocks subthreshold oscillations. *Neuron.* **81**, 1389–1400 (2014).

Acknowledgments

This work was support by research grants (No.11072132 and No.11272184) from National Natural Science Foundation of China.

Author contributions

H.C.Z., L.H.J. and Q.Y.Z. conceived the research, designed the experiments, prepared and revised the manuscript. Q.Y.Z. and J.X. performed the experiments. Y.Y.Z. and B.L.L. analyzed the data. S.N.L., B.H., C.X.L. and W.Y.C. provided technical support. All authors discussed the results and commented on the manuscript.

Additional information

Competing financial interests: The authors declare no competing financial interests.

How to cite this article: Zhang, Q.-Y. *et al*. Stiff substrates enhance cultured neuronal network activity. *Sci. Rep.* **4**, 6215; DOI:10.1038/srep06215 (2014).